Discriminating between the Role of Phase Matching and that of the Single-Atom Response in Resonance Plasma-Plume High-Order Harmonic Generation

Noa Rosenthal and Gilad Marcus
Department of Applied Physics, Hebrew University of Jerusalem, Jerusalem 91904, Israel
(Received 27 April 2015; published 22 September 2015)

Resonance enhancement of high-order harmonic generation has recently been found in the interaction of intense ultrashort laser pulses with laser ablated plasma plumes. It is a promising route towards the production of an intense and coherent extreme ultraviolet radiation source. However, the mechanism of this resonance enhancement is still not clear. There are two possible explanations; one relies on a better recombination cross section through an autoionization state in the single-atom response. The other relies on improved phase matching conditions around the resonance. Here, we try to discriminate between these two conjectures by measuring coherence lengths of the harmonics, both on resonance and off resonance. Our findings support the single-atom response hypothesis.

DOI: 10.1103/PhysRevLett.115.133901 PACS numbers: 42.65.Ky, 32.80.Wr, 78.47.jh

Introduction.—High-order harmonic generation emerges in the form of extreme ultraviolet (XUV) radiation when an intense ultrashort laser pulse interacts with a gas target. The process of high-order harmonic generation (HHG) is most intuitively explained through the well-known three-step model [1,2] in which the electron first tunnels out from the atom due to the strong electric field of the laser; it is then accelerated in the laser electric field and, when the electric field changes direction, the electron is pushed back to the parent ion with an excess of kinetic energy. The last step in this model is the recombination of the electron with the parent ion which is accompanied by the release of the excess energy in the form of an energetic photon typically carrying energies of a few tens of eV. High-order harmonics have been generated in atomic, molecular, and ionized gases [3–5]. The resulting harmonic spectra have a universal shape common to almost all the gases used [3]: it has a long plateau region in which the intensity of all the harmonics are almost identical, followed by a sharp drop called the cutoff energy. The universality of the harmonic spectra shape, together with the lack of small details which relate to the specific gas in use, suggest that the HHG process is nonresonant. A few years ago, it was discovered that HHG in some laser-ablated plasmas do show resonance features in the harmonic spectra [6–9]. These features are seen to coincide with a transition of an electron from an autoionization level back to the ground state of a single ionized atom [9]. Recently, resonance HHG has been discovered in other systems, for example, in atomic Fano resonances [10] and in SF6 molecule [11]. Resonance enhanced HHG introduces the possibility of increasing the conversion efficiency of a specific harmonic by more than an order of magnitude compared to nonresonant HHG in noble gases [12–14]. If this effect could be combined with phase-matching effects and/or coherent control of HHG, then an intense XUV source could be generated with only a single harmonic in the spectrum. Such a unique radiation source will truly be ideal for accelerating its various applications in physics, chemistry [15], biology, and for exploring new fields such as nonlinear x-ray optics [16] and in attosecond physics. It would have excellent spatial coherence [17], the possibility of high repetition rate (of the order of kilohertz to hundreds of kilohertz), and improved conversion efficiency.

There are two possible explanations for the mechanism of this resonant harmonic. The most common is based on modified three-step model. In this modified model, instead of recombining directly from the continuum to the ground state, the recolliding electron is first captured into an autoionization state of the same energy, and only then decays into the ground state while releasing a XUV photon [9,18,19]. However, a second explanation relies on the collective response of the medium instead of the single-atom response, i.e., on the phase matching conditions [17,20,21].

Phase matching refers to the constructive accumulation of radiation from coherent sources along the beam propagation direction. This condition translates to the condition $\Delta k = k_q - qk_0 = 0$, where Δk is the phase mismatch factor, k_q is the q^{th} harmonic wave vector, and k_0 is the fundamental wave vector. In the case of HHG, there are several physical processes that contribute to the phase mismatch term, and their relative importance is determined by the experimental conditions [22–25]. This phase mismatch factor can be written as:

$$\Delta k = \underbrace{\frac{q\omega_0}{c}(n_q - n_0)}_{\mathrm{I}} + \underbrace{\frac{2b(q-1)}{b^2+4z^2}}_{\mathrm{II}} + \underbrace{f(\vec{\nabla}U_p)}_{\mathrm{III}}, \quad (1)$$

where n_q and n_0 are the refractive indices of the q^{th} harmonic and the fundamental wave, respectively, b is the confocal parameter, and $U_p = [(eE)^2/4m\omega^2]$ is the

 © 2015 American Physical Society

ponderomotive energy. The three main contributions to the mismatch term are labeled as I, II, and III in Eq. (1), corresponding to the contributions from (I) the refractive indices, (II) the geometrical Gouy phase shift, and (III) the atomic phase accumulated while the electron traverses the continuum before it recombines with its parent ion [3,22,23]. It is well-known that the refractive index changes dramatically in the vicinity of a sharp and strong resonance. Therefore, it is possible to have better phase matching conditions for a certain harmonic near the resonance [17,20,21].

Beside the possibility of improving the performance of the harmonic sources, the resonant harmonic is interesting in itself as it involves the interaction between electrons and the possible interactions of valence electrons with inner shell electrons [26,27]. To date, the mechanism for this enhancement is still debatable but only few attempts have been made to discriminate between the two explanations. Haessler *et al.* performed the first temporal characterization of the envelope shape [28] and the attosecond emission [29] from tin plasma under near-resonance conditions by using the RABITT or reconstruction of attosecond beating by interference of two-photon transitions technique [30]. They found missing RABITT sidebands around the resonant harmonic and attributed the lack of those sidebands to the large phase shift across the resonant harmonic. However, such a strong phase shift could be explained either by the single-atom response or by the strong change in the refractive index across the resonance [17]. In this Letter, we describe a careful measurement of the coherence lengths of the harmonics from a laser-ablated chromium plasma for both the resonant harmonic (H29) and the off resonance harmonics. By examining how the coherence length of the resonance harmonic is related to the coherence lengths of its neighboring harmonics, we can assess the role that phase matching plays in resonance enhancement.

Experiment.—The experimental setup is schematically shown in Fig. 1. We begin by separating the uncompressed beam from our regenerative Ti:sapphire amplifier (1 kHz, 160 ps) into two beams. One of the beams (the pump beam) is used to heat the chromium target and generate the plasma medium. The second beam (the probe beam) is delayed by ≈45 ns with respect to the pump beam, compressed to about 30 fs and used to generate the harmonics from the chromium plasma. The uncompressed pump beam is focused onto a chromium solid plate inside a vacuum chamber. The chromium plate was placed on a motorized stage in order to refresh the target during the experiment. The pump beam is first line focused by a $f = 400$ mm cylindrical lens. An adjustable slit is placed at the focus of this lens and then imaged with a 5∶1 telescope onto the chromium surface to generate the chromium plasma. In this way, we can precisely control the chromium plasma length. The intensity of the pump beam on the chromium target is calculated to be in the range from 1.5×10^{10} to 2.5×10^{10} W/cm^2 by measuring the pulse energy, pulse duration, and spot area. The compressed probe pulse is focused with a plano-convex $f = 500$ mm lens on the chromium plasma and generates the high harmonics. Both the femtosecond beam and the harmonics continue propagating in the vacuum system. A 1500 nm thick aluminum filter blocks the femtosecond beam and allows only the harmonics to enter the spectrometer. The harmonic beam is dispersed by a 1200-grooves/mm grazing incidence reflective grating and is recorded by a back illuminated XUV CCD.

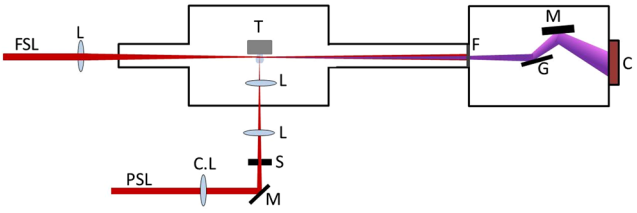

FIG. 1 (color online). Experimental setup for high harmonic generation in a plasma. The amplified 800 nm beam from the regenerative amplifier (4 mJ, stretched to 160 ps) is split into two beams. One is compressed to 30 fs (FSL: femtosecond laser) and used to generate the high harmonics; the second beam (PSL, picosecond heating pulse) is used to ablate the chromium plate and generate the plasma medium; C.L, cylindrical lens; L, lens; S, slit; M, mirror; T, Cr target for the plasma generation; F, aluminum filter; G, reflective grating; C, XUV CCD camera.

Results and Discussion.—Figure 2 shows a representative HHG spectrum from the Cr plasma. It is similar to the spectra that was reported in [8] and is obviously different from the typical HHG spectra. Instead, we can clearly see the enhancement of the 29th harmonic with respect to the neighboring harmonics. In order to determine the phase matching conditions for the different harmonics, we measured harmonic yield as a function of the interaction length. We control the interaction length between the harmonic generating beam and the Cr plasma by placing in the prepulse pathway an adjustable slit at the focal plane of the cylindrical lens. In this way, we affect the prepulse beam shape which results in a change in the plasma length. The plasma length as a function of the slit width was calibrated by placing a beam profiler at the position of the Cr target. The experimental results are presented in Fig. 3. Figure 3(a)

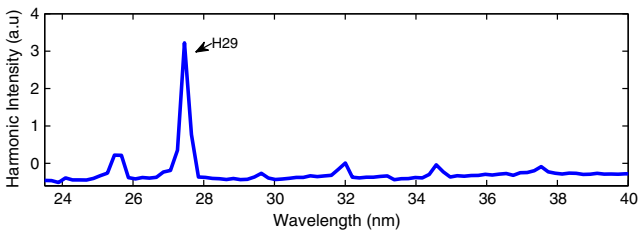

FIG. 2 (color online). Harmonic spectra from chromium plasma including the resonance harmonic (H29).

shows a false color map of the harmonic yield as a function of the interaction length. Figure 3(b) shows vertical lineouts of Fig. 3(a) for four representative harmonics. H23 and H25 are two off resonance harmonics below the resonance. H29 is the resonant harmonic and H31 is an off resonance harmonic above the resonance. The coherence lengths and the absorption lengths of the harmonics were inferred from the data by fitting the harmonic yield curves to Eq. (2) derived by E. Constants *et al.* [31]. It can be seen that even

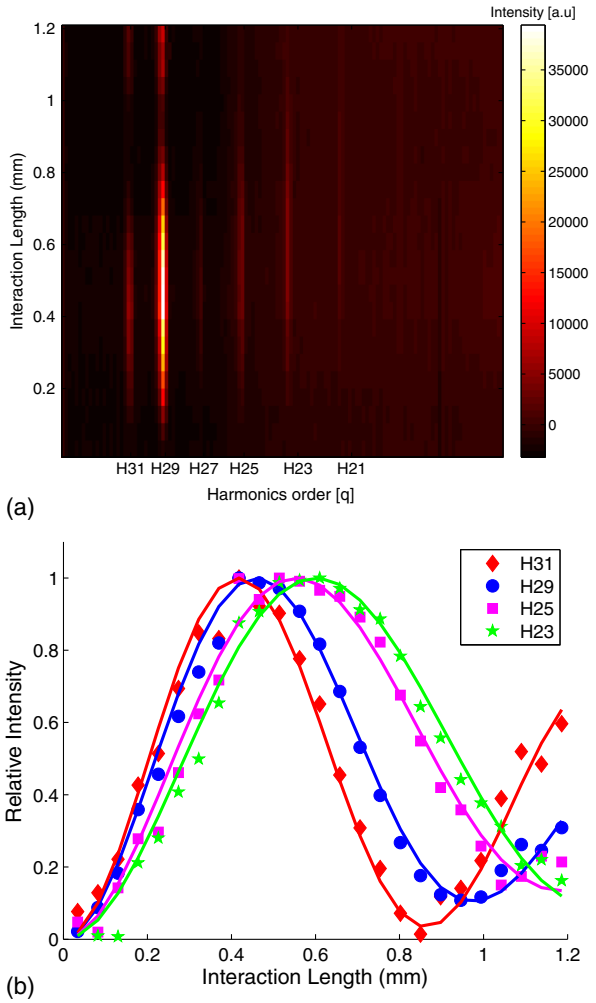

FIG. 3 (color online). Harmonic yield as a function of the Cr plasma length. We controlled the medium length by the procedure described above. Here, the pump beam intensity is 1.58×10^{10} W/cm^2. Figure 3(a) shows the harmonic yield as a false color map. The resonance harmonic (H29) is clearly enhanced over its neighboring harmonics. Figure 3(b) shows normalized vertical lineouts of the upper frame for different harmonics (H29 is the resonant harmonic, H31 above the resonance, H23 and H25 are below the resonance). The diamonds, circles, squares, and stars represent the experimental data, the solid lines are the fitting curves to the experimental data according to Eq. (2). By fitting the data to Eq. (2), we deduced the coherence lengths and the absorption lengths for the various harmonics. The fitted coherence lengths are given in Fig. 4.

though the intensity of the resonant harmonic is much higher than the intensity of the other harmonics, they all show the same pattern in relation to the variations in interaction length. All the harmonics, including the resonant harmonic, vary like a damped cosine function over the interaction length. The intensity of the harmonics keeps growing with the interaction length until the interaction length L_m is comparable to the coherence length $L_{\mathrm{coh}} = \pi/\Delta k$. Beyond the coherence length, destructive interference starts to play a role, and the harmonic yield drops. However, because of the absorption, complete cancellation of the signal usually is not achieved. After passing twice the coherence length, the constructive buildup starts to play a role again, and so on. This behavior is well described by the formula derived by E. Constant *et al.* [31] [Eq. (2)].

$$N_{\mathrm{out}} \propto \frac{4L_{\mathrm{abs}}^2 (A_q \rho)^2}{1 + 4\pi (L_{\mathrm{abs}}/L_{\mathrm{coh}})^2} \times \cdots \times \left[1 + \exp\left(-\frac{L_m}{L_{\mathrm{abs}}}\right) - 2\cos\left(\frac{\pi L_m}{L_{\mathrm{coh}}}\right) \exp\left(-\frac{L_m}{2L_{\mathrm{abs}}}\right)\right]. \quad (2)$$

Here, N_{out} is the number of photons emitted on axis per unit of time and area, L_{abs} is the absorption length, L_{coh} the coherence length, L_m the medium length, A_q is the amplitude of the atomic response at the harmonic frequency, and ρ is the plasma density. Using this equation, both the coherence length and the absorption lengths are found to be of the same order of magnitude, about 500 micron. The coherence lengths of the various harmonics for two different pump intensities are presented in Fig. 4.

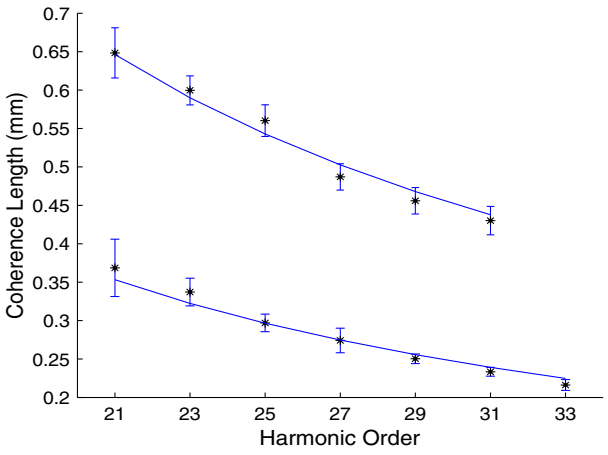

FIG. 4 (color online). Fitted coherence length vs the harmonic order for two pump laser intensities, i.e., for two different plasma densities (upper curve: $I_p = 1.58 \times 10^{10}$ W/cm^2, lower curve: $I_p = 2.56 \times 10^{10}$ W/cm^2). The points are the fitted coherence lengths, the error bars are the 95% confidence limits, and the solid lines are fit curves α/q where α is a fitting scaling parameter and q is the harmonic order. It clearly shows that the coherence lengths follow the $1/q$ trend in accordance with Eq. (1).

Figure 4 summarizes the results of our study. It shows a smooth change in the coherence length as a function of the harmonic order q with a power law of q^{-1}. This trend is what one would expect from the phase mismatch term given by Eq. (1) if parts I and II are the dominnant parts. To further determine whether dispersion or geometrical phase mismatch dominate in our experiment, we repeated our experiment but this time with almost twice as much higher pump intensity, i.e., with increased plasma density. If the geometrical term in Eq. (1) is dominant, we should see no effect on coherence length. However, if the dispersion term is dominant, we should see a reduction of the coherent lengths due to the higher medium density. The results of our control experiment confirm that dispersion is the dominant effect which determines the coherent lengths (see Fig. 4). By assuming that plasma dispersion is the main contribution to the medium dispersion and using measured coherent length, we calculated the plasma density to be $\approx 1\text{–}2 \times 10^{17}$ cm^{-3} for pump intensities $1.58\text{–}2.56 \times 10^{10}$ W/cm^2, in agreement with previously reported works on HHG from plasma plumes [32].

Conclusions.—Our results, given in Figs. 2 and 3(a), clearly indicate the existence of a resonance enhanced harmonic in our spectrum. Nevertheless, analysis of coherence length does not show any dramatic change in the coherence length of that harmonic with respect to the neighboring harmonics. Our results do not support the phase matching enhancement hypothesis. Rather, it favors the viewpoint that the single atom is responsible. However, the single-atom response not fully understood, and further investigation must be carried on.

This research was supported by the Israel Science Foundation (Grant No. 404/12).

[1] J. L. Krause, K. J. Schafer, and K. C. Kulander, Phys. Rev. Lett. **68**, 3535 (1992).
[2] P. B. Corkum, Phys. Rev. Lett. **71**, 1994 (1993).
[3] P. Salières and M. Lewenstein, Meas. Sci. Technol. **12**, 1818 (2001).
[4] H. Sakai and K. Miyazaki, Appl. Phys. B **61**, 493 (1995).
[5] P. Arpin, T. Popmintchev, N. L. Wagner, A. L. Lytle, O. Cohen, H. C. Kapteyn, and M. M. Murnane, Phys. Rev. Lett. **103**, 143901 (2009).
[6] R. A. Ganeev, L. B. Elouga Bom, J. C. Kieffer, and T. Ozaki, Phys. Rev. A **75**, 063806 (2007).
[7] R. A. Ganeev, H. Singhal, P. A. Naik, and P. D. Gupta, Quantum Electron. **37**, 827 (2007).
[8] R. A. Ganeev, P. A. Naik, H. Singhal, J. A. Chakera, and P. D. Gupta, Opt. Lett. **32**, 65 (2007).
[9] R. Ganeev and P. Redkin, Opt. Commun. **281**, 4126 (2008).
[10] J. Rothhardt, S. Hädrich, S. Demmler, M. Krebs, S. Fritzsche, J. Limpert, and A. Tünnermann, Phys. Rev. Lett. **112**, 233002 (2014).
[11] A. Ferré *et al.*, Nat. Commun. **6**, 5952 (2015).
[12] M. Suzuki, M. Baba, R. Ganeev, H. Kuroda, and T. Ozaki, Opt. Lett. **31**, 3306 (2006).
[13] L. B. Elouga Bom, R. A. Ganeev, J. Abdul-Hadi, F. Vidal, and T. Ozaki, Appl. Phys. Lett. **94**, 111108 (2009).
[14] R. A. Ganeev, T. Witting, C. Hutchison, F. Frank, P. V. Redkin, W. A. Okell, D. Y. Lei, T. Roschuk, S. A. Maier, J. P. Marangos, and J. W. G. Tisch, Phys. Rev. A **85**, 015807 (2012).
[15] Y. Nabekawa, Y. Furukawa, T. Okino, A. Amani Eilanlou, E. J. Takahashi, K. Yamanouchi, and K. Midorikawa, Sci. Rep. **5**, 11366 (2015).
[16] P. Tzallas, E. Skantzakis, L. A. A. Nikolopoulos, G. D. Tsakiris, and D. Charalambidis, Nat. Phys. **7**, 781 (2011).
[17] R. A. Ganeev, T. Witting, C. Hutchison, V. V. Strelkov, F. Frank, M. Castillejo, I. Lopez-Quintas, Z. Abdelrahman, J. W. G. Tisch, and J. P. Marangos, Phys. Rev. A **88**, 033838 (2013).
[18] V. Strelkov, Phys. Rev. Lett. **104**, 123901 (2010).
[19] P. V. Redkin, M. K. Kodirov, and R. A. Ganeev, J. Opt. Soc. Am. B **28**, 165 (2011).
[20] R. A. Ganeev, Open Spectrosc. J. **3**, 1 (2009).
[21] I. A. Kulagin, V. V. Kim, and T. Usmanov, Quantum Electron. **41**, 801 (2011).
[22] P. Balcou and A. L'Huillier, Phys. Rev. A **47**, 1447 (1993).
[23] P. Balcou, P. Sali'eres, A. L'Huillier, and M. Lewenstein, Phys. Rev. A **55**, 3204 (1997).
[24] S. Kazamias, D. Douillet, F. Weihe, C. Valentin, A. Rousse, S. Sebban, G. Grillon, F. Augè, D. Hulin, and P. Balcou, Phys. Rev. Lett. **90**, 193901 (2003).
[25] C. G. Durfee, A. R. Rundquist, S. Backus, C. Herne, M. M. Murnane, and H. C. Kapteyn, Phys. Rev. Lett. **83**, 2187 (1999).
[26] G. Marcus, W. Helml, X. Gu, Y. Deng, R. Hartmann, T. Kobayashi, L. Strueder, R. Kienberger, and F. Krausz, Phys. Rev. Lett. **108**, 023201 (2012).
[27] A. D. Shiner, B. E. Schmidt, C. Trallero-Herrero, H. J. Worner, S. Patchkovskii, P. B. Corkum, J. C. Kieffer, F. Legare, and D. M. Villeneuve, Nat. Phys. **7**, 464 (2011).
[28] S. Haessler, L. B. Elouga Bom, O. Gobert, J. F. Hergott, F. Lepetit, M. Perdrix, B. Carré, T. Ozaki, and P. Salières, J. Phys. B **45**, 074012 (2012).
[29] S. Haessler, V. Strelkov, L. B. Elouga Bom, M. Khokhlova, O. Gobert, J. F. Hergott, F. Lepetit, M. Perdrix, T. Ozaki, and P. Salières, New J. Phys. **15**, 013051 (2013).
[30] P. M. Paul, E. S. Toma, P. Breger, G. Mullot, F. Augé, P. Balcou, H. G. Muller, and P. Agostini, Science **292**, 1689 (2001).
[31] E. Constant, D. Garzella, P. Breger, E. Mevel, C. Dorrer, C. Le Blanc, F. Salin, and P. Agostini, Phys. Rev. Lett. **82**, 1668 (1999).
[32] R. Ganeev, M. Suzuki, M. Baba, and H. Kuroda, Appl. Phys. B **81**, 1081 (2005).